Screening effects in nuclear fusion of hydrogen isotopes in dense media

Néstor R. Arista* and Alberto Gras-Martí
Departament de Física Aplicada, Universitat d'Alacant, Apartat 99, E-03080 Alacant, Spain

Raúl A. Baragiola
Department of Physics and Astronomy and Laboratory for Surface Modification, Rutgers University, Piscataway, New Jersey 08855-0849
(Received 25 July 1989)

Nuclear-fusion rates of isotopic hydrogen nuclei embedded in dense screening media are calculated. We consider the cases of a uniform degenerate electron gas and the inhomogeneous electron density in solids. We derive an exact wave function for the screened nuclear interaction and an analytical expression for the barrier-penetration factor in the case of homogeneous screening. For qualitative estimates of the screening in solids, we use a Thomas-Fermi description of the electron density. A crossover of the fusion rates of the various isotopic pairs analyzed (*p-d*, *d-d*, *p-t*, and *d-t*) is predicted for increasing screening length, velocity, or effective temperature of the medium. The effects of variable screening length and local effective temperatures are considered for electron gases in the range of metallic densities and compared with previous experimental and theoretical studies.

I. INTRODUCTION

As is well known, recent publications have reported experiments that seemed to indicate the feasibility of achieving cold-fusion reactions in electrochemical[1] or pressure[2] cells, with metals containing large concentrations of hydrogen isotopes. These findings, however, are contradicted by recent careful experiments.[3] Significant experimental effort is currently in progress to check the proposed schemes or other reaction channels and conditions. At any rate, the necessity has been apparent to reevaluate existing theoretical models of fusion reactions of hydrogen isotopes in dense screening media. One would like to understand and quantify, for instance, the role played by the solid matrix where the eventually fusing nuclei are thought to react. Also needed are predictions for fusion rates under conditions not considered so far in sufficient detail. On the other hand, electron screening effects are also of interest for thermonuclear reactions occurring in astrophysical plasmas.[4–6]

We present here a calculation of nuclear fusion rates of hydrogen isotopes embedded in a uniform electron gas and in the inhomogeneous electron distribution of a solid matrix. In both cases, the screening due to the electron background provides a means to overcome with higher probability the repulsive Coulomb barrier between the reacting isotopes.

First we analyze the effects of screening on the probability of tunneling through the repulsive barrier. We treat the two-body screened interaction between the isotopes by means of a model repulsive potential that renders itself to analytical evaluation for the *s* component of the wave function.

The barrier-penetration factor is calculated for the main hydrogenic fusion reactions in a homogeneous electron gas, with a screening parameter determined by the density of the background electrons. To study fusion reactions in solids, and for order-of-magnitude estimates, we use a Thomas-Fermi description of the electron density, and furthermore assume statistical distributions of isotopes in phase space, with variable screening lengths within the volume of the atomic cell. We discuss predictions of the present model for *d-d*, *p-d*, *p-t*, and *d-t* reactions in homogeneous screening media, and in nonhomogeneous electron gases at metallic densities.

II. FUSION RATES IN A HOMOGENEOUS ELECTRON GAS

We start by analyzing the fusion probability of hydrogenic nuclei immersed in a uniform screening medium such as a homogeneous electron gas. The fusion rate between two nuclei can be calculated from[7]

$$\Gamma = A|\psi(0)|^2 , \tag{1}$$

where Γ is the number of fusion processes occurring per second, and A is a constant whose value depends on the specific fusion reaction considered. The wave function $\psi(r)$ for the relative motion of the two fusible nuclei that interact via a potential $U(r)$ is determined from the Schrödinger equation

$$\nabla^2\psi(r) = -\frac{2\mu}{\hbar^2}[E - U(r)]\psi(r) , \tag{2}$$

where $E = \mu v^2/2$, v is the relative velocity of the nuclei, and μ is their reduced mass.

In the following we shall consider a screened repulsive interaction between the free nuclei, as given by the Hulthén potential:[8]

$$U(r) = \frac{e^2 q_0}{(e^{q_0 r} - 1)} , \tag{3}$$

where the screening parameter q_0 will be specified below.

 ©1989 The American Physical Society

This potential permits to obtain analytical solutions for the s-wave components of the wave function, and thus allows to derive an exact result for the probability density at the origin $|\psi(0)|^2$, which occurs in Eq. (1). The potential in Eq. (3) was introduced by Hulthén[8] to evaluate the bound states of the neutron-proton system and was later used[9] to study the density *enhancement factor* in the scattering of free electrons by the attractive potential of a nucleus.

For the present case of a repulsive potential, Eq. (2) can be written for s states in the form

$$\phi''(\xi)+\lambda^2\phi(\xi)=\frac{g\phi(\xi)}{e^{\xi}-1} , \tag{4}$$

with $\xi=q_0 r$, $\phi(\xi)=r\psi(r)$, and

$$\lambda=\frac{\mu v}{\hbar q_0} , \tag{4'}$$

where $g=2\mu e^2/\hbar^2 q_0$ is twice the ratio of the screening length to the Bohr radius for a system of reduced mass μ.

After transforming the radial coordinate in Eq. (4) to the variable $z=1-e^{-\xi}$, we find that the solution for the s state of the two isotopes takes the form

$$\phi(\xi)=(1-e^{-\xi})\exp(-i\lambda\xi)F(\alpha,\beta,2,1-e^{-\xi}) , \tag{5}$$

where $F(\alpha,\beta,\gamma,z)$ is the hypergeometric function,[10] with $\alpha=1+i(\delta+\lambda)$, $\beta=1-i(\delta-\lambda)$, and $\delta=(\lambda^2+g)^{1/2}$. The parameters α and β are functions of the relative velocity v and the screening constant q_0 [see Eq. (4')].

Taking the limits of the hypergeometric function[10] in Eq. (5) for $r=0$ and $r\Longrightarrow\infty$, we find an exact expression for the *attenuation factor* (or barrier-penetration factor) χ, which accounts for quantum-mechanical tunneling across the repulsive nuclear barrier, i.e.,

$$\chi(q_0,v)=\frac{|\psi(0)|^2}{|\psi(\infty)|^2}=\frac{2\pi e^2}{\hbar v}G(\lambda,\delta) , \tag{6}$$

where the Gamow factor G is exactly given by

$$G(\lambda,\delta)=\frac{e^{-2\pi(\delta-\lambda)}(1-e^{-4\pi\lambda})}{(1-e^{-2\pi(\delta+\lambda)})(1-e^{-2\pi(\delta-\lambda)})} . \tag{7}$$

In the appropriate limit, $q_0\Longrightarrow 0$, the Gamow factor reduces to the well-known result for a pure Coulomb repulsive potential,[11]

$$G(\infty,\infty)=\frac{1}{e^{2\pi v_0/v}-1} , \tag{7'}$$

where $v_0=e^2/\hbar$ is Bohr's velocity.

From Eqs. (6) and (1), the fusion rate is

$$\Gamma_\sigma=A\chi(q_0,v)n_\sigma , \tag{8}$$

where $n_\sigma=|\psi(\infty)|^2$ is the density of nuclei in the medium. We shall later let $\sigma=p$, d, or t, for protons, deuterons, or tritons, respectively.

Equation (8) gives the fusion rate, *per scattering center*, for a flux $n_\sigma v$ of nuclei. For a density $n_{\sigma'}$ of scattering centers we calculate the fusion rate, *per unit volume* of the medium embedding the isotopes, in the form

$$\gamma_{\sigma\sigma'}=\Gamma_\sigma n_{\sigma'}=A\chi(q_0,v)n_\sigma n_{\sigma'} . \tag{9}$$

As will become apparent below, the fusion rate in Eqs. (8) or (9) shows a very strong dependence on the relative velocity v and the screening parameter q_0, due to the form of $\chi(q_0,v)$, Eq. (6).

It will be more convenient in the following to work in atomic units (a.u.), with $e=m=\hbar=1$. Lengths are then measured in units of Bohr's radius $a_0=0.529$ Å, and temperatures in Ry (27.2 eV or $\sim 3\times 10^5$ K).

In the case of a degenerate (homogeneous) electron gas, for instance, the so-called Thomas-Fermi screening constant is given by

$$q_0=\sqrt{3}\frac{\omega_p}{v_F} , \tag{10}$$

where $\omega_p=(4\pi n_e)^{1/2}$ and $v_F=(3\pi^2 n_e)^{1/3}$ are the plasma frequency and the Fermi velocity, respectively, for an electron gas of density n_e.

The one-electron radius r_s describing the electron density is defined from $(4\pi/3)r_s^3=1/n_e a_0^3$. Typically r_s is ~ 2 for metals (1.51 for solid Pd), ~ 0.6 for the Jupiter core, ~ 0.3 for the plasma at the center of the Sun, and ~ 0.01 for white dwarfs.

We also note that for some astrophysical applications one may need to account for the effects of partial degeneracy on the screening properties of the electron gas. This can be accomplished by using a more general expression for the screening constant, as given for all temperatures in Refs. 4 and 12.

In the high-electron-density limit, a relativistic correction to the screening constant must be introduced. From the long-wavelength limit of the static dielectric constant[13] one gets a correction factor $(1+v_F^2/c^2)^{1/4}$ in the right-hand side of Eq. (10). In the nonrelativistic range, $q_0\simeq 1.56/r_s^{1/2}$.

In Fig. 1 we show the values of $A\chi(q_0,v)$ for interacting p-d and d-d pairs for various energies of relative motion and for a range of screening parameters that includes the various r_s of interest mentioned above. The constant A was taken from Refs. 7 and 14. As can be observed in Fig. 1, the fusion rates for p-d and d-d reactions depend very strongly on the screening conditions and on the collision energy. While p-d fusion rates are larger for low screening and low energies, d-d fusion takes over in the opposite limits. This crossover will be discussed below. As expected, the screening of the charge of the fusing nuclei by the electron gas can lead to differences in the fusion rates of many orders of magnitude.

The highest values of q_0 (~ 200 a.u.) correspond to strongly screened interactions, as they would apply, for instance, for bound p-μ or d-μ muonic systems[15] studied in muon-catalyzed fusion reactions. In fact, and as one could anticipate on physical grounds, the large variations of χ for various screening conditions are similar to those found[15,14] for bound deuterium molecules, though using a different approach pertinent to bound states of the reacting isotopes and, in Ref. 14, introducing a variable effective electron mass.

We can estimate the fusion rates of different isotopic pairs, for instance, p-d and d-d. Taking, for simplicity, equal densities for each isotope, $n_p=n_d=n_0$, and using

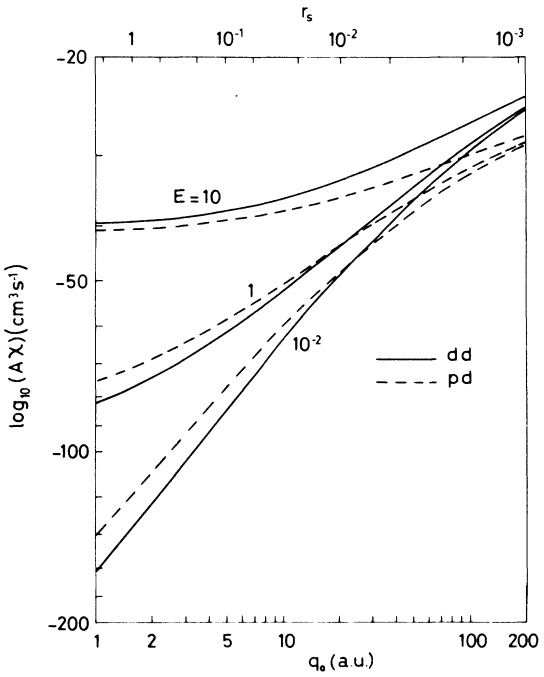

FIG. 1. Barrier-penetration factor $\chi(q_0,v)$ (weighted with the nuclear reaction constant A) for a homogeneous electron gas, Eq. (6), as a function of the reciprocal screening length q_0 or related electron-gas density (upper scale). E is the center-of-mass energy of the fusing nuclei in a.u. Solid lines, d-d reactions; dashed lines, p-d reactions.

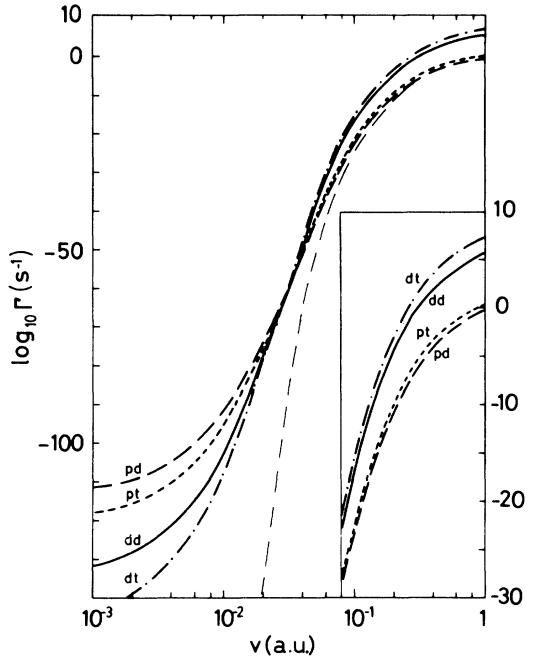

FIG. 2. Fusion rates from Eqs. (11a) and (11b) vs the relative velocity v of the isotopes for reacting protons (p), deuterons (d), and tritons (t) in a homogeneous electron gas with $q_0=1.27$ a.u. (corresponding to solid Pd). The light-dashed curve is the p-d fusion rate in the absence of screening.

Eq. (9), we define the following fusion rates, per isotopic pair:

$$\Gamma_{pd}=\frac{\gamma_{pd}}{n_0}=A\chi n_0\ , \tag{11a}$$

$$\Gamma_{dd}=\frac{\gamma_{dd}}{n_0/2}=2A\chi n_0\ . \tag{11b}$$

In Fig. 2 we show fusion rates for the main isotopic combinations, in a uniform electron gas of density corresponding to that of solid Pd, as a function of the relative velocity of the isotopes. We have taken an isotopic concentration $n_0=10^{23}$ nuclei/cm^3, corresponding to average solid-state densities. A drastic increase in the fusion rate (even in a log scale) is observed for increasing energies of the interacting nuclei. At low velocities, the magnitude of the fusion rate is found to be larger the lower the reduced mass μ of the nuclei. In this velocity range the tunneling probability, depending on the factor $\chi(q_0,v)$ in Eqs. (6) and (7), is a strongly decreasing function of μ. In the opposite limit of high velocities, $\chi\Longrightarrow 1$ and the fusion rates reorder according to the values of the reaction constant A, which increases with μ.

The p-d fusion rate neglecting screening ($q_0=0$), shown as a light dashed curve in Fig. 2, indicates that screening becomes increasingly important for $v<0.1$ a.u. ($\sim$200 eV for p-d or d-d reactions).

For simplicity of the discussion, we shall consider in the following only p-d and d-d reactions. In Fig. 3 we show fusion rates averaged over relative velocities, assuming a thermal (Maxwell-Boltzmann) distribution of

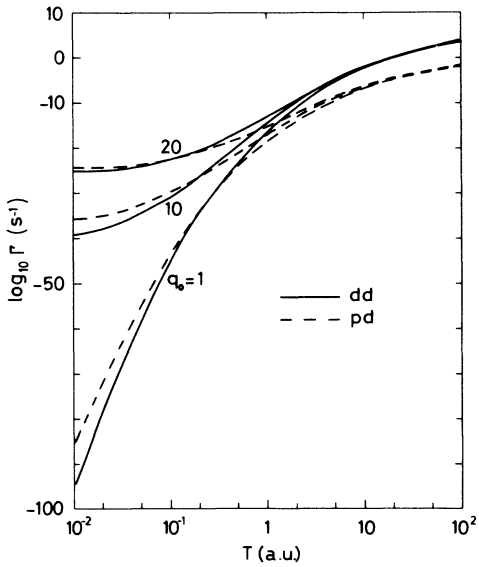

FIG. 3. Fusion rates for p-d and d-d reactions in a homogeneous electron gas as a function of temperature T. q_0 is the screening constant (in a.u.) and $n_0=10^{23}$ cm^{-3}.

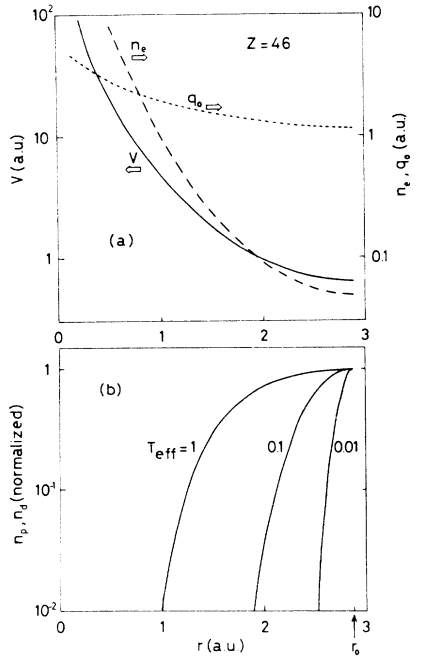

FIG. 4. (a) Spatial profiles of electron density n_e, screening parameter q_0, and the TF potential V for Pd. (b) Spatial profiles of hydrogen isotopes within the WS cell defined by $r_0=2.88$ a.u. normalized to the same value of the concentration at the border of the cell. $T_{\rm eff}$ is the effective temperature (in a.u.).

isotopes and for three values of the screening constant q_0. The largest effect of temperature on the fusion rates is found for $q_0\simeq 1$ a.u., which is a typical value of the screening constant in metals.

III. NONHOMOGENEOUS SYSTEMS

The previous analysis applies to the question of nuclear fusion of hydrogen isotopes under the presence of screening effects in a dense, but otherwise homogeneous electron gas. To explore the possibility of fusion catalyzed by solids, we need to consider additionally the effects of inhomogeneities both in the spatial distribution of the isotopes and in the electron density in the solid. We apply here a description based on the statistical Thomas-Fermi (TF) model to represent the spatial variation of the electronic distributions and calculate fusion rates for confined atomic systems in a solid.[16]

Consider a Wigner-Seitz (WS) cell of radius r_0 around a lattice position in a solid, with an average interatomic distance $1.61r_0$ (with $r_0\sim 2.88$ a.u. for solid Pd). The electron-density distribution $n_e(r)$ and the atomic potential $V(r)$ generated around each matrix atom, are determined from the differential TF equation, $d^2\varphi/dx^2=\varphi^{3/2}x^{-1/2}$, for the TF screening function $\varphi(x)$. $V(r)=Ze^2\varphi(r/a)/r$, $a=0.8853Z^{-1/3}$ in a.u., Z is the atomic number of the matrix atom, and $n_e=(32Z^2/9\pi^3)[\varphi(x)/x]^{3/2}$. We use the confined-atom model to evaluate numerically the TF potential.

The fusion rate in Eq. (9) is now integrated over the spatial and velocity distributions of the colliding nuclei to yield

$$\Gamma_{\sigma\sigma'}=A\int d^3r\int d^3v_\sigma\int d^3v_{\sigma'}\chi(r,|\mathbf{v}_\sigma-\mathbf{v}_{\sigma'}|)\times n_\sigma(r,v_\sigma)n_{\sigma'}(r,v_{\sigma'})\ , \qquad (12)$$

where $v=|\mathbf{v}_\sigma-\mathbf{v}_{\sigma'}|$ is the relative velocity of the two isotopes having individual velocities $\mathbf{v}_\sigma$ and $\mathbf{v}_{\sigma'}$. For the presently considered nonhomogeneous screening, the attenuation factor χ in Eq. (12) is a function of position of the isotope with respect to the matrix atom and of the relative velocity of the interacting nuclei. The spatial dependence arises because in our local-density approximation the screening parameter q_0, Eq. (10), changes with the position occupied by the isotope in the electron cloud of the matrix atom.

The densities of the isotopes in phase space will be described by a Maxwell-Boltzmann statistical distribution, characterized by an effective temperature $T_{\rm eff}$, namely,

$$n_\sigma(r,v_\sigma)=C_\sigma\exp\{-[\tfrac{1}{2}m_\sigma v_\sigma^2+\Delta V(r)]/(kT_{\rm eff})\}\ , \qquad (13)$$

Where m_σ is the nuclear mass, $\Delta V(r)=V(r)-V(r_0)$, and C_σ is a normalization constant.

Then, the two integrals over velocities, appearing in Eq. (12), can be reduced to a single integration over the relative velocity $\mathbf{v}$, in the form

$$\Gamma_{\sigma\sigma'}=A\int d^3r\, n_\sigma(r)n_{\sigma'}(r)\int d^3v\,\chi(r,v)f_{\rm MB}(v)/v_{\rm th}^3\ , \qquad (14)$$

where $f_{\rm MB}$ is now the Maxwell-Boltzmann velocity distribution for a particle of mass μ, $v_{\rm th}=(2kT_{\rm eff}/\mu)^{1/2}$ is the most probable thermal relative velocity, and $n_\sigma(r)$ is obtained by integration of the density in Eq. (13) over all velocities.

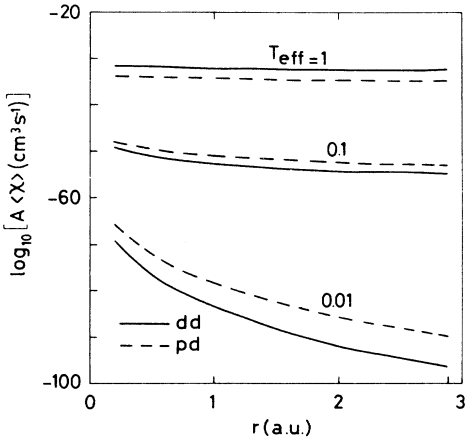

FIG. 5. Spatial dependence of the thermally averaged attenuation factor χ, Eq. (17), for a local TF model of solid Pd. Solid lines, d-d reactions; dashed lines, p-d reactions. The parameter on the curves is the effective temperature (in a.u.).

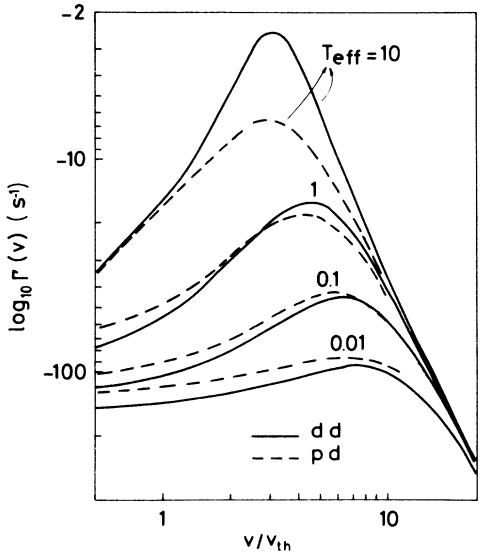

FIG. 6. Velocity-dependent fusion rate $\Gamma(v)$ defined by Eqs. (18) and (18′) for a TF model of solid Pd, where $v_{th}=(2kT_{eff}/\mu)^{1/2}$. Solid lines, *d-d* reactions; dashed lines, *p-d* reactions. T_{eff} is the effective temperature (in a.u.).

In order to normalize the fusion rates in a standard way, we calculate the number of p or d nuclei in the WS cell,

$$N_\sigma=\int d^3r\, n_\sigma(r)\ , \tag{15}$$

and finally obtain the *average fusion rate per p-d or d-d pair* in the medium, as follows:

$$\bar{\Gamma}_{\sigma\sigma'}=\frac{\Gamma_{\sigma\sigma'}}{N_0}\ , \tag{16}$$

where N_0 is the number of pairs. In the *p-d* case, N_0 is taken as the smallest of N_p and N_d (for a 50% mixture of p and d, $N_0=N_p=N_d$), while for the *d-d* case, $N_0=N_d/2$.

We show in Fig. 4 the input quantities in the model, $n_e(r)$, $q_0(r)$, $V(r)$, $n_p(r)$ and $n_d(r)$. One sees that all the quantities, except the screening parameter, undergo large changes within the atomic cell in the solid. The largest variations occur for the concentration of the isotopes, especially at low temperatures.

Now we evaluate, for the present model, the attenuation factor entering Eq. (14), averaged over the velocity distribution, viz.

$$\langle\chi\rangle=\int d^3v\,\chi(r,v)f_{MB}(v)/v_{th}^3\ . \tag{17}$$

As shown in Fig. 5, the spatial dependence of this velocity-averaged fusion rate is smooth, except for the lowest temperatures. Again, just as we observed for a homogeneous screening medium, the relative significance of *p-d* or *d-d* reactions shifts at different temperature ranges.

The same qualitative conclusion regarding the weight of the *p-d* or the *d-d* reactions is obtained from a spatial average of the fusion rate. Figure 6 shows the quantity

$$\bar{\Gamma}_{\sigma\sigma'}(v)=\frac{4\pi}{N_0}\left[\frac{v}{v_{th}}\right]^2 f_{MB}(v)A\int d^3r\, n_\sigma(r)n_{\sigma'}(r)\chi(r,v)\ , \tag{18}$$

which gives the contribution at each velocity to the total fusion rate of Eq. (16),

$$\bar{\Gamma}_{\sigma\sigma'}=\int\bar{\Gamma}_{\sigma\sigma'}(v)\frac{dv}{v_{th}}\ . \tag{18′}$$

There is, at each temperature, a range of velocities where the contribution to the fusion rate is maximum, and this range broadens and shifts towards increasing velocities for decreasing effective temperature. In all cases, the maximum contribution to the fusion rates comes from the high-velocity tails of the Maxwell-Boltzmann distributions.

Table I shows integrated fusion rates for *p-d* and *d-d* reactions, Eq. (18′), for $n_0=10^{23}$ nuclei/cm^3, and for several temperatures T_{eff}. In comparing the rates in Table I one notes that at low temperatures the *p-d* reaction is most probable, but for increasing T_{eff} the *d-d* reaction becomes dominant for mixtures containing comparable concentrations of isotopes. A similar crossing of the fusion rates was predicted in Ref. 14 in terms of an *ad hoc* variable effective mass for the electrons. The transition from *p-d* to *d-d* favorable reaction occurs at $T_{eff}\cong 0.1$ a.u. At low temperatures, the calculated fusion rates are very much lower than the values estimated from the experiments of Ref. 1. The rates predicted by the present model are also smaller than those obtained[15] using a molecular description for bound hydrogenic isotopes. However, the existence and characteristics of bound states, when the isotopes are immersed in a metal, are currently subjects of investigation. Using a different formalism[17] it was previously found that H_2 is not bound in jellium for $r_s<2$, while recent calculations[18] show that the distance between the hydrogen isotopes in a palladium matrix becomes still larger than for molecular hydrogen in the gas phase.

TABLE I. Fusion rates (in s^{-1}) from Eq. (16) for $n_0=10^{23}$ nuclei/cm^3 and several effective temperatures T_{eff}. (Note: A temperature of 0.01 a.u. corresponds to $kT_{eff}\sim 0.27$ eV or $T_{eff}\sim 3000$ K.) The dominant reaction at each temperature is marked with an asterisk.

T_{eff} (a.u.)	10^{-2}	10^{-1}	1	10	10^2
$\log_{10}(\bar{\Gamma}_{pd})$	−84.0*	−42.7*	−18.2	−6.4	−1.2
$\log_{10}(\bar{\Gamma}_{dd})$	−94.0	−44.5	−16.0*	−2.5*	+3.6*

If one were to use the present model to reach the *cold*-fusion rates 10^{-23}–10^{-20} s^{-1} claimed in Ref. 1, one would require local temperatures of the order of 1 a.u. It is not clear to us whether one could expect a significant increase in local temperatures, or other kinetic effects, under the conditions of these experiments.

IV. SUMMARY AND CONCLUSIONS

We have considered the calculation of nuclear fusion rates of isotopic hydrogen nuclei in a dense screening medium, in particular for a homogeneous electron gas and for the inhomogeneous electron distributions in solids. The effect of the screening is to increase the probability of barrier penetration for a repulsive potential and is described by the attenuation factor $\chi(q_0,v)$ in Eq. (6). An analytical calculation of χ was performed for the Hulthén repulsive potential. The variation of $\chi(q_0,v)$ was studied for the main fusion reactions between protons, deuterons, and tritons for screening conditions corresponding to a dense electron gas in ranges of interest for fusion studies in solids or astrophysical applications.

A crossover of the fusion rates for *p-d*, *p-t*, *d-d*, and *d-t* reactions is predicted as a function of velocity, temperature, or screening conditions. For instance, the predicted fusion rates for *p-d* reactions are larger at low temperatures, while the *d-d* reaction rates become larger at high temperatures. These results may be considered in qualitative agreement with the findings of Ref. 14. The main difference between this and other models[15,14] is that our approach considers the scattering of nearly free nuclei in a dense screening medium, while the previous model[15] was developed for the case of bound molecular states, as they form in the gas phase. Hence the predictions of the present model apply, in general terms, under conditions that may be of interest for various physical or astrophysical fusion studies.

For the screening conditions in metals, the screening effects become important for energies below ~200 eV in the *p-d* and *d-d* cases. Fusion rates of the order of those reported in recent experiments[1] (10^{-23}–10^{-20} s^{-1}) cannot be explained by the present model unless considerably high effective temperatures are assumed. On the other hand, the dramatic increase of the fusion rates with effective temperature (cf. Table I) may encourage the use of alternative techniques to try to achieve local heating of the hydrogen isotopes embedded in solids. One can, for instance, recall the intense heating effects occurring in inertial-confinement fusion experiments. Thus, we conclude that the alternative model presented here, appropriate for dense screening media, may be useful for fusion-rate estimates in different experimental situations.

ACKNOWLEDGMENTS

We acknowledge discussions with P. M. Echenique, E. Louis, F. Moscardó and E. San-Fabián. The present collaboration has been possible through a sabbatical stay of Néstor Arista sponsored by the Spanish Ministerio de Educación y Ciencia. Partial support from the DGICYT is recognized (Project No. PS 88-0066).

*On leave from Centro Atómico Bariloche, RA-8400 SanCarlos de Bariloche, Rio Negro, Argentina.

[1] M. Fleischmann and S. Pons, J. Electroanal. Chem. **261**, 301 (1989); S. E. Jones, E. P. Palmer, J. B. Czirr, D. L. Decker, G. L. Jensen, J. M. Thorne, S. F. Taylor, and J. Rafelski, Nature **338**, 737 (1989).

[2] A. De Ninno, A. Frattolillo, G. Lollobattista, L. Martinis, M. Martone, L. Mori, S. Podda, and F. Scaramuzzi, Europhys. Lett. **9**, 221 (1989).

[3] J. F. Ziegler, T. H. Zabel, J. J. Cuomo, V. A. Brusic, G. S. Cargill, III, E. J. O'Sullivan, and A. D. Marwick, Phys. Rev. Lett. **62**, 2929 (1989).

[4] E. E. Salpeter, Aust. J. Phys. **7**, 373 (1954).

[5] H. J. Assenbaum, K. Langanke, and C. Rolfs, Z. Phys. A **327**, 461 (1987).

[6] C. Rolfs, H. P. Trautvetter, and W. S. Rodney, Rep. Prog. Phys. **50**, 233 (1987).

[7] J. D. Jackson, Phys. Rev. **106**, 330 (1957).

[8] L. Hulthén, Ark. Mat. Astron. Fys. **28A**, 1 (1942).

[9] J. Lindhard and A. Winther, Nucl. Phys. **A166**, 413 (1971).

[10] *Handbook of Mathematical Functions*, edited by M. Abramowitz and I. A. Stegun (Dover, New York, 1965).

[11] L. D. Landau and E. M. Lifshitz, *Quantum Mechanics: Non-Relativistic Theory* (Pergamon, New York, 1977).

[12] N. R. Arista and W. Brandt, Phys. Rev. A **29**, 1471 (1984).

[13] B. Jancovici, Nuovo Cimento **25**, 428 (1962); I. Nagy, J. Phys. B **19**, L421 (1986).

[14] S. E. Koonin and M. Nauenberg, Nature **339**, 690 (1989).

[15] C. D. Van Siclen and S. E. Jones, J. Phys. G **12**, 213 (1986).

[16] N. R. Arista, J. Phys. C **19**, L841 (1986); N. R. Arista and A. R. Piriz, Phys. Rev. A **35**, 3450 (1987).

[17] J. K. Norskov, Phys. Rev. **20**, 446 (1979). He finds, using the Kohn-Sham density-functional formalism, a very small attractive interaction between protons (not present in the Hulthén description) only for very low electron densities ($r_s = 3.93$).

[18] Z. Sun and D. Tománek, Phys. Rev. Lett. **63**, 59 (1989); J. W. Mintmire, B. I. Dunlap, D. W. Brenner, R. C. Mowrey, H. D. Ladouceur, P. P. Schmidt, C. T. White, and W. E. O'Grady (unpublished).